TAE No. 463

AD A111964

Repeated Buckling Tests
of Stiffened Thin Shear Panels

by

J. Ari-Gur

J. Singer

A. Libai

DTIC
SELECTED
MAR 1 2 1982
B

Scientific Report No. 1

82 08 12 019

Best
Available
Copy

TAE 463

ERRATA

p.2   line 6:   "..Thurlmann.."   should read: "..Thurliman.."

       line 8:   "..Scalsud.."   should read: "..Scaloud.."

       line 13:   should read: (c/b) = 0.2

p.3   line 17:   should read: "..aircraft that.."

p.4   line 7:   should read: $N = 2 \times 10^5$

       line 3 from bottom: "..text.." should read "..test.."

p.8   line 11:   should read: "..panel , to.."

p.11 line 5:   should read: "..certain.."

       last line: "..flagne.."   should read "..flange.."

p.12 line 4:   should read: "..loading.."

p.17 line 10:   should read: "..observations.."

Ref. 11:   "..Thurlmann.." should read: "..Thurliman.."

Refs. 12, 13, 14: "..Scalond.." should read: "..Scaloud.."

Ref. 34: "..Hansner.." should read: "..Hausner..".

REPEATED BUCKLING TESTS OF STIFFENED THIN SHEAR PANELS

by

J. Ari-Gur

J. Singer

A. Libai

Department of Aeronautical Engineering

Technion - Israel Institute of Technology

Haifa, Israel

ABSTRACT

An experimental study of repeated buckling of shear panels, which represents the first phase of a more comprehensive program is presented. Two similar typical Wagner beams were tested under cyclic loading not exceeding 70% of the predicted ultimate static load, one tested as a cantilever and one loaded symmetrically at three points. The aim of these pilot tests was better understanding of the physical phenomena and evaluation of the experimental methods for future tests. The appropriate location and precautions for use of strain gages to measure the stress concentrations at the edges of the diagonal of tension were determined, and the suitability of the shadow moiré technique for deflection measurements was ascertained. It was found that cyclic loading at a fairly high load level causes significant structural changes in the shear panels that affect the failure of the beam.

Accession For

NTIS CRA&I

DTIC TB

A

-i-

TABLE OF CONTENTS

NOTATION

b distance between stiffeners (Fig. 1)

C coefficient, Eq. (1)

c distance from stiffener to plastic hinge of flange failure (Fig. 1)

D distance between camera and light source

d overall height of beam (Fig. 1)

I_f area moment of inertia of flange cross-section

L distance of camera and light source from plane of panels

N number of cycles

n fringe number

p wave length of moire grid

S stress level of cyclic loading

S_b bending stress level of cyclic loading

t web thickness

V external shear force

V_{cr} external shear force at initiation of web buckling

V_u ultimate external shear force

w out-of-plane deflection of panel

β angle of rotation of flange at failure (Fig. 1)

θ_t angle of diagonal tension

σ_t diagonal tensile stress

τ_{cr} shear stress for initiation of web buckling

τ_u ultimate shear stress

1. INTRODUCTION

Stiffened plates are widely used in many engineering applications, especially in aircraft, ships and civil engineering structures. The stable post-buckling behavior of plates and the large increase in buckling loads that is achieved by attachment of stiffeners are most advantageous to the designer. When loaded in shear, the stiffened plate shows high post-buckling strength, first explained by Wilson [1] in 1886. He observed "that when stiffeners were properly introduced, the web no longer resisted by compression, but by tension, the stiffeners taking up the duty of compressive resistance." This idea is the basis of the "diagonal tension" theory developed by Wagner in 1929 [2] for very thin sheet and rigid reinforcements. The theory of "pure diagonal tension" was later extended to "incomplete diagonal tension" theory, and both were summarized in a convenient manual [3] with test results [4] and in Kuhn's book [5] or Hertel's book [6]. Whereas in the "pure diagonal tension" theory the web is considered as inclined tension members in a frame, the extended theory takes into account the compressive stresses in the plate and its reinforcing contribution to the stiffeners. The results of the "pure diagonal tension" theory are reasonable for loads exceeding the initial buckling load of the panel by at least an order of magnitude.

Extensive studies on steel plate girders were reported by many civil engineering investigators [7-24]. In a review of the ultimate load methods for prediction of the failure loads of plate girders, Rockey [7] states that "aircraft structures normally fail when the web plate tears, whereas the steel plate girders used in civil engineering have more flexible flanges and fail by either the development of plastic mechanisms involving the web and the flanges

or by lateral buckling of the compression flanges." The diagonal tension theory, adequate for aircraft structures, is therefore insufficient for civil engineering, where the ratio (V/V_{cr}) of applied load to critical load of panel buckling is practically less than four. During the last two decades theories were developed for failure of civil engineering-type plate girders. The extreme assumption of Basler and Thurbmann [8-11] that the flanges are so flexible that they cannot withstand lateral loading, was modified by Rockey and Skalsud [14] to a more realistic one. They assumed that the flexural rigidity of the flanges contributes to the strength of the girder and plastic hinges are developed in the flanges when failure occurs (Fig. 1). Their method is substantiated by extensive test data. They found that the location (c/b) of the central plastic hinge depends on the flange stiffness ratio (I/b^3t), ranging from (c/b) 0.2 for very flexible flanges to (c/b) = 0.5 for very stiff ones. It should be noted here that the effect of the flexural stiffness of the flanges on the post-buckling behavior of the panel is very significant. It affects primarily the stress distribution and the depth of the inclined buckling waves.

Deep buckling waves are obtained in girders with flexible flanges, when the following condition, proposed by Rockey [15], is satisfied:

$$\frac{I_f}{b^3t} \leq C(\frac{V}{V_{cr}} - 1) \tag{1}$$

The coefficient C depends on the panel aspect ratio, and it varies from 10^{-5} and 2×10^{-5} for (b/d) = 1.0 and 1.2 to 32×10^{-5} and 35×10^{-5} for (b/d) = 2.0 and 3.0, respectively. For a given structure, Eq. (1) provides the maximum external shear force (V) that may be applied with relatively shallow buckling

waves in the web.

One should remember that the flexibility of the flanges also affects the initial buckling of the shear web. This effect has been studied theoretically [17-19] and experimentally [4], and correction coefficients appear in the usual calculations [3].

The trend to optimize the design of plate girders in civil engineering and stiffened shear panels in aeronautical engineering leads to similar required relative stiffnesses in both fields. Civil engineers build with stiffer flanges in order to improve the postbuckling strength of the web, while aeronautical engineers decrease the relative flange cross-section area in order to save weight (see, for example, [20]). There are obviously considerable differences in materials, methods of manufacturing, stiffeners spacing and in service conditions, but it appears that more interaction between these disciplines is now appropriate and may be very beneficial.

The objective of the present investigation is to study the post-buckling behavior and fatigue failue of stiffened slender plates subjected to repeated shear buckling. Service failures of aircraf tht could be attributed to repeated buckling and the insufficient attention given to this topic have motivated the present study. The authors of [3] commented that "it has been found experimentally that a load in excess of the buckling load will cause a lowering of the buckling stress for the next application of the load" and therefore they anticipated that for repeated loading "failure will take place at a lower load than predicted." The advance of plate girder design in civil engineering from buckling-limit design ($V/V_{cr} \leq 1$) to post-buckling general collapse design, that resulted in high bending stresses of the web, promoted studies of the initiation and propagation of fatigue cracks in large steel plate girders, like those of bridge constructions, which are subjected to

periodic loads. Yen and Mueller [21,22] observed that cracks initiated in the web along the flanges in regions of the highest bending stresses. They plotted S-N curves for their results and obtained reasonable S-N behavior only when the bending stress (S_b) was plotted versus N. In these tests and other civil engineering investigations [23,24] the maximum load applied did not exceed 3.5 V_{cr} (and about half the static strength) and fatigue cracks appeared after more than N-2 10^5 cycles.

Typical aircraft shear web beams are designed for service at load ratios larger than (V/V_{cr}) = 3.5. The deep inclined buckling waves result in large curvature of the web and repeated buckling may cause fatigue failure. In a recent study on composite (graphite/epoxy) shear webs [25] a considerable reduction in the initial buckling load due to fatigue was observed, but in two out of three panels the ultimate strength was not affected.

It should be noted that in these tests the webs were stiffened with relatively stiff stiffeners and rigid flanges. Periodic loading of an amplitude of approximately 60% of the ultimate failure load (V/V_{cr} = 5.6) caused delaminations of stiffeners from the web in the tension field corners after 2×10^4 cycles but the loading was continued without additional damages and terminated at 5×10^5 cycles. In another specimen a crack started after 5×10^4 cycles and propagated steadily The loading was stopped at 2.5×10^5 because of the large cumulative damage.

Another study of aluminum alloy shear webs, representing modern fighter wings [26], subjected to similar cyclic loading (V/V_{cr} ≈ 6), also showed initiation of cracks at points of high bending stress. The fatigue life observed in the text was 1.45×10^5 cycles and agreed reasonably well with the estimated one, based on S-N curves for the material, indicating that the ultimate strength was reduced due to fatigue.

The theoretical efforts have been aimed both at calculation of post-buckling deformations and at prediction of life estimates from calculations of maximum bending stresses arising at the edges of the deep diagonal buckles. Early analytical studies of the post-buckling behavior of shear panels [27,28] were not conclusive. More recently, computer codes like NASTRAN [29], STAGS [30] and others were employed by several investigators (see, for example, [25,22,26,31-33] to calculate post-buckling deflections and stresses of a single loading, and compare the results with those from available experiments. The results of the post-buckling bending stresses were then used to predict cracking of the web through available S-N results of the material. Fair correlation was obtained [22,26] for predictions based on bending fatigue data.

It may be noted that in the case of composite shear panels even the calculation of the buckling load is complicated and numerical procedures may have to be resorted to (see for example [34]).

The effects of stiffener-web interaction on fatigue behavior at high load ratios (V/V_{cr}) was not considered in [25] or in the other tests reported in the literature. In design applications this parameter may, however, be important. For example, in a typical shear web made of composite material in a modern fuselage [35] the load ratios for repeated buckling was about 27.

Moreover, there is a lack of data on the variations of post-buckling behavior due to the cyclic loading. In the present report two pilot tests on riveted aluminum alloy Wagner beams are described. The research project is continued in order to study the influence of repeated shear buckling on the post-buckling behavior and durability of stiffened shear web beams with different structural configurations.

2. TEST SPECIMENS

Two beams were tested. Both specimens, of 2024-T3 aluminum alloy, have similar flange, stiffeners and webs (designated by F, S and W, respectively, in Fig. 2). The net dimensions of a panel are 270 mm x 180 mm, with web thickness t = 0.5 mm resulting in an aspect ratio (d/b) = 1.5 and a slenderness (b/h) = 360. The flanges and the stiffeners are riveted to the web on both sides in symmetric pairs. Each flange (two L40 x 40 x 4) has $I_f \approx 9.5 \times 10^4$ mm^4. Hence the flange stiffness ratio ($I_f/b^3 t$) is 0.0326, which is two or three orders of magnitude larger than that of common civil engineering plate girders, but represents a typical thin web aircraft-type structure, a typical Wagner beam. The vertical stiffeners are pairs of L20 x 20 x 1.

The elastic shear buckling stress of the panels, calculated by the procedure proposed in Section 4.2 of [3], is τ_{cr} = 5.35 N/mm^2, and the corresponding external shear force is, therefore, V_{cr} = 900 N, assuming that shear is carried by the web only.

For the ultimate shear stress of τ_u = 203 N/mm^2 of the 2024-T3 aluminum alloy web, the nominal external shear load for web rupture is 34.1 kN, but this value should be corrected since, due to flange flexibility, stress concentrations occur at the edges of the panels. For the present beam the external shear load should accordingly be decreased by 11% (see [3], Sec. 4.7), and the predicted ultimate external force is therefore V_u = 31 kN.

The major differences between the specimens WB=01 and WB-02 are in the conditions of support and loading: WB-01 was fixed at one edge and loaded at the other (Fig. 3), whereas WB-02 was supported at both edges and loaded in the central section (Fig. 4). The symmetry of the second specimen results in

two identical short cantilevers fully clamped at the center. On the other

hand, the attachment of the cantilever WB-01 is not completely rigid and its

length results in larger bending moments.

3. METHODS OF MEASUREMENT

Since the main objective of the investigation is to study the effects of repeated buckling on the fatigue process, the changes in the behavior of the panels due to cyclic loading had to be measured.

3.1 Strain Measurement

Strain gage rosettes were bonded to the Wagner beams at several web locations. In specimen WB-01 five pairs of strain rosettes were attached – one at the center of the panel and four at its corners (See Fig. 3). Pairs of axial strain gages were employed to measure strains at four locations of the stiffeners and flanges. In Wagner beam No. 2 strains were only measured in the web near the diagonal tension edges and at the center of the panel.to study stress distributions near an edge. Three pairs of strain rosettes were located at the diagonal tension/tension flange corner (see Fig. 4) in order to study stress distributions near an edge. Hence, a total of 38 strain records were obtained in the test of WB-01 and 30 for WB-02, the channels being scanned by as B&F multi-channel recorder, modified for digital output.

3.2 Deflection Measurements

Strain measurements have three major disadvantages: 1) Data are restricted to the point of measurement. 2) To obtain extensive data excessive instrumentation is necessary. 3) Results do not provide information on buckling pattern and deflections. The results obtained by strain gages should therefore be complemented by other methods, and here the shadow-moiré method was preferred. With this relatively simple technique successive topographical views of the deflected panel are obtained, the buckling pattern is clearly

visible and areas of large curvatures and bending stresses are identified. Whereas in Wagner Beam No. 1 (WB-01) only the deflections of a single panel were measured by this technique, in WB-02 the deflections of both panels were measured by it.

To simplify the calibration of the moire pattern fringes the grid was positioned very close to the web (not more than 1 cm) and the light source and the camera were positioned far away from the beam (more than 100 cm) both at the same distance from the plane of the panels. For the specimen WB-01, a grid of 20 lines per centimeter, or wavelength of p = 0.05 cm, was employed, and the light source and camera were L = 115 cm away from the specimen and D = 190 cm apart. An approximate calibration formula

$$\frac{\Delta w}{\Delta n} \simeq p \frac{L}{D} \tag{2}$$

yielded 0.03 cm/fringe and the actual calibration against a controlled central deflection (measured with a micrometer) yielded 0.034 cm/fringe. In WB-02 two different grids were used, p_1 = 0.05 cm and p_2 = 0.025 cm, in panels 1 and 2, respectively. With the distances L=286 cm and D = 286 cm, calibrations of 0.050 and 0.025 cm/fringe were predicted. The actual calibration, obtained in the same manner as in WB-01, correlated well with the prediction.

It should be noted here, however, that deflection measurement alone would not be sufficient, since it does not provide information on in-plane stresses. Moreover, the shadow-moire technique is not very sensitive ($\sim\pm0.1$ mm) and the accuracy of bending strains found by this method is much lower than that obtained by strain gages. Hence a combination of deflection measurement and judiciously located strain gages is required.

Another method of deflection measurement is by a Linear Variable Differential Transformer (L.V.D.T.) normal to the web. This instrument is very sensitive (± 0.01 mm) and accurate deflection readings are obtained. Deflections were scanned by means of L.V.D.T. travelling along an inclined line of the panel (see Figs. 3,4) crossing the direction of the shear buckling waves, in order to verify the wave numbers and the magnitudes of the deflections observed by the moiré pattern.

4. TEST PROCEDURE AND RESULTS

Test procedures for both specimens were, in general, similar:

a) positioning and calibration.

b) slow gradual loading up to V_{max} with measurements of strains and deflections at certan intermediate load levels, and release of loading.

c) cyclic loading between $V = 0$ and $V = V_{max}$, with several interruptions after certain numbers of cycles, to repeat the procedure of slow gradual loading and intermediate measurements, to examine the specimens and evaluate the apparent changes in structural behavior.

4.1 Specimen WB-01

After positioning, instrumentation and calibration, Wagner Beam No. 1 (see Fig. 5) was loaded from $V = 0$ to $V = 11.77$ kN, in intervals of 1.96 kN, for measurement of strains (38 channels) and deflections (by photography of moirè patterns and by travelling L.V.D.T.). After load release this procedure was repeated. V_{max} was then increased to 13.73 kN, and eight cycles of slow loading were applied with complete measurements of strains and deflections.

The main results observed during this phase were:

a) diagonal buckling wave fringes became visible from $V \approx 1.6$ kN.

b) The repeated loading from $V = 0$ to $V_{max} = 13.73$ kN did not produce any changes in the buckling pattern or in the unloaded shape.

c) At the edges of the diagonal of tension residual strains appeared. Due to bending their magnitudes at similar locations on opposite sides of the web were significantly different. The maximum residual strain after these ten cycles of slow loading appeared on the web at the corner of the panel near the compression flagne. Its magnitude, in the

principal direction of 21° from the flange, was 526με, whereas on the opposite side it was 258με with 29° inclination.

In the second phase, cyclic loading with V_{max} = 13.73 kN was applied at a loaing frequency of 2-3 cycles per minute up to 10400 cycles. The cyclic loading was interrupted several times, and a slow loading with complete measurements was carried out. Two channels of strain gages were recorded continuously during the cyclic loading.

During this phase, residual deflections at the web (Fig. 6) changed the initial buckling pattern (Fig. 7) but did not significantly affect the patterns at higher load levels (V ⌐ 7.85 kN). Residual strains were notably increased, and, at the corner near the compression flange, they exceeded 15000με on one side but did not reach 2000με on the opposite side. These residual strains were, therefore, caused primarily by bending.

In the third phase of loading the external shear force was increased to V_{max} = 19.62 kN and additioanl 1000 load cycles were applied. The increase of load level resulted in a change of buckling pattern from 6-7 half-waves at V = 13.73 kN to 8 half-waves at V = 19.62 kN (Fig. 8). Additional plastic deformation was caused, but the 1000 cycles up to this load level did not affect the buckling pattern.

In the last phase the Wagner Beam No. 1 was loaded statically to failure at V_u = 23.0 kN. The failure pattern is presented in Fig. 9. Cracks occurred at the corners of the diagonal of tension near the tension flange where the web was torn by the tensile forces.

4.2 Specimen WB-02

Wagner Beam No. 2 (see Fig. 10) was first loaded statically to V = 13.73 kN and released, then to V_{max} = 19.62 kN and released and later to V_{max} =

21.58 kN. For each loading complete measurements were carried out at several load levels and after release.

The main results observed during the first phase of loading were:

a) A diagonal buckling wave pattern became visible in panel 2 (the sensitive moiré grid) at V ≈ 0.9 kN, and at V ≈ 1.20 kN more waves appeared (see Fig. 11a).

b) Relatively large residual deformations appeared already after the first loading (V = 13.73 kN). The growth of residual deflections after each static loading level is presented in Fig. 12. The largest residual strains appeared at the corner of the diagonal of tension near the compression flange. Their values after each loading and release are presented in Table 1. All these strains are in the direction of compression, perpendicular to the direction of diagonal tension.

TABLE 1. Residual Strains After Three Slow Loadings at Corner of Diagonal Tension/Compression Flange

Load Released From	Largest Bending		Largest Inplane	
	Strain [µε]	Direction	Strain [µε]	Direction
V = 13.73 kN	830	-50°	-360	-50°
V = 19.62 kN	4450	-54°	-1550	-54°
V = 21.58 kN	6780	-55°	-2030	-55°

Note: Positive direction is measured at this corner from the flange into the web.

In the second phase of loading after the first three slow loadings, cyclic loading (10 cycles/minute) between $V = 0$ and $V_{max} = 21.58$ kN was applied until failure. Although final failure occurred at $N = 6750$ cycles, considerable changes in structural behavior were observed already from $N = 2085$ onwards. The initial residual deflection pattern of the cyclic phase of loading (see Fig. 12-c) remained unchanged until $N = 2085$ when unloading caused snapping of the web into a distorted smeared plastic wave (Fig. 13). From this point gradual changes occurred in the unloaded pattern of panel 1, and at $N = 6010$ a crack was observed at the edge of the diagonal of tension near the compression flange. The crack (Fig. 14) started at the edge of the buckling wave along its peak, in the general direction of the tension field. This crack is obviously a result of the high bending stresses at the sharp fold of the wave near the edge of the panel. Another branch of the crack was in the direction perpendicular to the tension field. These cracks branched out later along the stiffener and to the nearby panel, and the test was terminated at $N = 6750$ cycles, when the Wagner Beam No. 2 was not capable anymore to carry V_{max}. The final failure pattern is pesented in Fig. 15.

Strain concentrations and strain distribution were also studied. At $V = 21.58$ kN the diagonal tension strain at the center was approximately 3500 µε, independently of the number of load cycles. Close to the upright stiffener similar tensile strains were observed. Close to the tension flange (near the diagonal tension corner) these strains were always smaller by about 20% and they increased very slowly with N. The tensile strain at the corner showed significant dependence on the number of cycles only after $N = 2085$, when the residual deflection pattern changed. Before that it stayed steadily close in magnitude to the central average of 3500 µε. On the other hand, strain concentrations of 1.2-1.3 appeared at the corner near the compression flange

even before N = 2085. In the compressive direction stress concentrations were much larger (up to 1.7 was measured), exept near the upright stiffener.

5. <u>DISCUSSION AND CONCLUSIONS</u>

Two similar Wagner beams were tested under cyclic loading at load levels not exceeding 70% of the predicted ultimate load. The first specimen (WB-01) was of a cantilever-type, whereas the second (WB-02) was symmetrically loaded at three points.

Since the present pilot tests were only the first phase of a comprehensive research program on Wagner beams, they were aimed also at examination and selection of the appropriate test methods. The following conclusions were drawn on the experimental techniques employed:

a) Severe bending strains and strain concentrations occur at the edges of the diagonal of tension, and therefore strain gage rosettes should be bonded at these corners as close as possible to the junction of the stiffeners. Reference rosettes are also required at the center. Other gages on the web surface are unnecessary.

b) It is recommended to position the strain gage rosettes so that the perpendicular gages will be in the directions of the diagonal tension and normal to it. Each gage in every rosette should exactly face its partner on the opposite side.

c) The shadow-moiré technique yields sufficiently accurate and sensitive results. A travelling or scanning L.V.D.T. is therefore unnecessary. It is desirable to use the moiré technique on both panels with two different grid densities. At low levels of loading the dense grid is essential to detect the initiation of buckling and measure the relatively small deflections. Fig. 11-a shows the importance of this sensitivity. It is possible that the initial buckling load of WB-01 was lower than the observed one but the moiré pattern there was not

sensitive enough to identify it. At the high load levels, where very close fringes are obtained with the sensitive grid, the other one is more convenient for deflection measurement.

d) The method of loading at three points is preferable to the cantilever type since the boundary conditions are defined more precisely and no effects of flexibility of fixture have to be considered. It is possible that the differences in behavior between specimens WB-01 and WB-02 are the result of the different boundary conditions of the beams.

Though the results are not yet sufficient for definitive conclusions about the physical phenomena, the following general observatins can be made:

e) Calculation of web buckling according to [3] correlates well with experiments.

f) In both beams cyclic loading caused structural changes in the panels.

g) The specimen WB-01, which was loaded at a lower load level than WB-02, did not fail in cyclic loading.

h) The static failure of WB-01, which occurred after the cyclic loading procedure had been completed, took place at a static load considerably below the predicted failure load. The web was torn in tension.

i) In the initial stages of cyclic loading, stress concentrations occurred only at the corner of the panel near the compression flange.

j) The occurrence of changes in the residual deflection pattern in the panels of WB-02 was followed by redistribution of strain near the tension flange corner and large concentrations developed later at the edges.

k) In specimen WB-02 failure was due to cyclic loading, and it was initiated by a bending crack in the web at the peak of the buckling wave near the compression flange.

The research continues with emphasis on shear web beams with significantly lower flange to web stiffness ratios.

ACKNOWLEDGEMENTS

REFERENCES

1. Wilson, J.M., "On Specifications for Strength of Iron Bridges," Trans. ASCE, Vol. 15, Part I, 1886, pp. 401-403, 489-490.

2. Wagner, H., "Ebene Blechwandträger mit sehr dünnem Stegblech," Zeitschrift fur Flugtechnik und Motorluftsch., Vol. 20, Nos. 8,9, 10, 11, 12, 1929, translation: "Flat Sheet Metal Girders with Very Thin Metal Web," NACA TM Nos. 604-606, 1931.

3. Kuhn, P., Peterson, J.P. and Levin, L.R., "A Summary of Diagonal Tension, Part I - Methods of Analysis," NACA TN 2661, May 1952.

4. Kuhn, P. Peterson, J.P. and Levin. L.R., "A Summary of Diagonal Tension, Part II - Experimental Evidence," NACA TN 2662, May 1952.

5. Kuhn, P., Stresses in Aircraft and Shell Structures, McGraw-Hill, New York 1956.

6. Hertel, H., Leichtbau, Springer, Berlin/New York, 1960.

7. Rockey, K.C., "The Design of Web Plates for Plate and Box Girders - A State of the Art Report," in Steel Plated Structures, Dowling, P.J., Harding, J.E. and Frieze, P.E., eds. Crosby Lockwood Staples, London, 1977, pp. 459-485.

8. Basler, K., "Strength of Plate Girders," Ph.D. Thesis, Lehigh University, 1959.

9. Basler, K., "Strength of Plate Girders in Shear," J. Struct. Div., Proc. ASCE, VOl. 87 (ST7), October 1961, pp. 151-180.

10. Basler, K., "Strength of Plate Girders Under Combined Bending and Shear," J. Struct. Div., Proc. ASCE, Vol. 87 (ST7), October 1961, pp. 181-197.

11. Basler, K. and Thurlmann, B., "Strength of Plate Girder in Bending," Proceedings ASCE, Vol. 87 (ST7), October 1961, pp. 181-197.

12. Skalond, M., "Design of Webplates of Steel Girders with Regard to the Postbuckling Behaviour-Approximate Solution," The Structural Engineer, Vol. 40, No. 9, September 1962, pp. 270-284.

13. Skalond, M., "Design of Webplates of Steel Girders with Regard to the Postbuckling Behaviour-Analytical Solution," The Structural Engineer, Vol. 40, No. 12, December 1962, pp. 409-416.

14. Rockey, K.C. and Skalond, M., "The Ultimate Load Behaviour of Plate Girders Loaded in Shear," The Structural Engineer, Vol. 50, No. 1, January 1972, pp. 29-48.

15. Rockey, K.C., "Plate Girder Design - Flange Stiffness and Web Plate Behaviour," Engineering, 20n December 1957, pp. 788-792.

16. Porter, D.M., Rockey, K.C. and Evans, H.R., "The Collapse Behaviour of Plate Girders Loaded in Shear," The Structural Engineer, Vol. 53, No. 8, August 1975, pp. 313-325.

17. Stein, M. and Fralich, R.W., "Critical Shear Stress of an Infinitely Long Simply Supported Plate with Transverse Stiffeners," NACA TN 1851, 1949.

18. Cook, I.T. and Rockey, K.C., "Shear Buckling of Clamped and Singly-Supported Infinitely Long Plates Reinforced by Transverse Stiffeners," The Aeronautical Quarterly, Vol. 13, February 1962, pp. 41-69.

19. Rockey, K.C. and Cook, I.T., "Shear Buckling of Clamped and Simply-Supported Infintely Long Plates Reinforced by Transverse Stiffeners and a Central Longitudinal Stiffener," The Aeronautical Quarterly, Vol. 13, May 1962, pp. 95-114.

20. Jenkins, W.M., de Jesus, G.C. and Burns, A., "Optimum Design of Welded Plate Girders," The Structural Engineer, Vol. 55, No. 12, December 1977, pp. 547-553.

21. Yen, B.T. and Mueller, J.A., "Fatigue Tests of Large-Size Welded Plate Girders," Welding Research Council Bulletin No. 118, November 1966.

22. Mueller, J.A. and Yen, B.T., "Girder Web Boundary Stresses and Fatigue," Welding Research Council Bulletin, No. 127, January 1968.

23. Patterson, P.J., Corrado, J.A., Huang, J.S. and Yen, B.T., "Fatigue and Static Tests of Two Welded Plate Girders," Welding Research Council Bulletin No. 155, October 1970.

24. Parsanejed, S. and Ostapenko, A., "On the Fatigue Strength of Unsymmetrical Steel Plate Girders," Welding Research Council Bulletin, No. 156, November 1970, pp. 48-59.

25. Agarwal, B.L., "Postbuckling Behavior of Composite Shear Webs," AIAA Paper No. 80-0689 presented at the 21st Structures, Structural Dynamics and Materials Conf., Seattle, May 1980, Technical Papers, Part 1, pp. 210-218.

26. Ivanson, S., Jarfall, L., Samuelson, A. and Gamziukas, V., "Nonlinear Analysis of a Rectangular Panel Subjected to Shear Loads," The Aeronautical Research Institute of Sweden, Report FFA HU-1893, August 1976.

27. Koiter, W.T., "Het schnifplooiveld bij grote oversshrijdingen van de knikspanning (The post buckling behaviour of flat rectangular panels in shear and compression) N.L.L. Rep. S295 Nat. Aero. Res. Inst. Amsterdam 1944 (in Dutch).

28. Leggett, D., "The Stresses in Flat Panel Under Shear When the Buckling Load has been Exceeded," H.M. Stationery Office, R M No. 2430, 1950.

29. McCormick, C.W. (ed), "The NASTRAN User's Manual, NASA SP-222(01), Washington, D.C., 1973.

30. Almroth, B.D., Brogan, F.A., Meller, E., Zale, F. and Petersen, H.T., "Collapse Analysis for Shells of General Shape: User's Manual for the STAGS-A Computer Code," AFFDL TR-71-8, March 1973.

31. Stein, M. and Starnes, J.H., "Numerical Analysis of Stiffened Shear Webs in the Postbuckling Range," Numerical Solution of Nonlinear Structural Problems, Hartung, R.F. (ed.), ASME, November 1973, pp. 211-223.

32. Vestergren, P. and Knutsson, L., "Theoretical and Experimental Investigations of the Buckling and Post Buckling Characteristics of Flat Carbon Fibre Reinforced Plastic (CFRP) Panels Subjected to Compression or Shear Loads," ICAS 1978, Proceedings of the 11th Congress of the International Council of the Aeronautical Sciences, Singer, J. and Staufenbiel, R. (eds), Lisboa, Portugal, Sept. 1978, pp. 217-223.

33. Samuelson, L.A., Vestergren, P., Knutsson, L., Wangb g, K.G. and Gamziukas, V., "Stability and Ultimate Strength of Carbon Fiber Reinforced Plastic Panels," Proceedings of International Congress on Composite Materials (ICCM/3), Paris, August 1980, pp. 327-341.

34. Stein, M. and Hansner, J.M., "Application of Trigonometric Finite Difference Procedure to Numerical Analysis of Compressive and Shear Buckling of Orthotropic Panels," Computers and Structures, Vol. 9, 1978, pp. 17-25.

35. Foreman, C.R., "Design Concepts for Composite Fuselage Structures," Fibrous Composites in Structural Design, Lenoe, E.M., Oplinger, D.W. and Burke, J.J. (eds.), Plenum Press, New York, 1980, pp. 103-123.

36. Calladine, C.R., "A Plastic Theory for Collapse of Plate Girders under Combined Shearing Force and Bending Moment," The Structural Engineer, Vol. 51, No. 4, April 1973, pp. 147-154.

LIST OF FIGURES

Fig. 1   Failure mechanism for ultimate design of plate girders [14].

W - WEB (t = 0.5 mm)
F - FLANGE
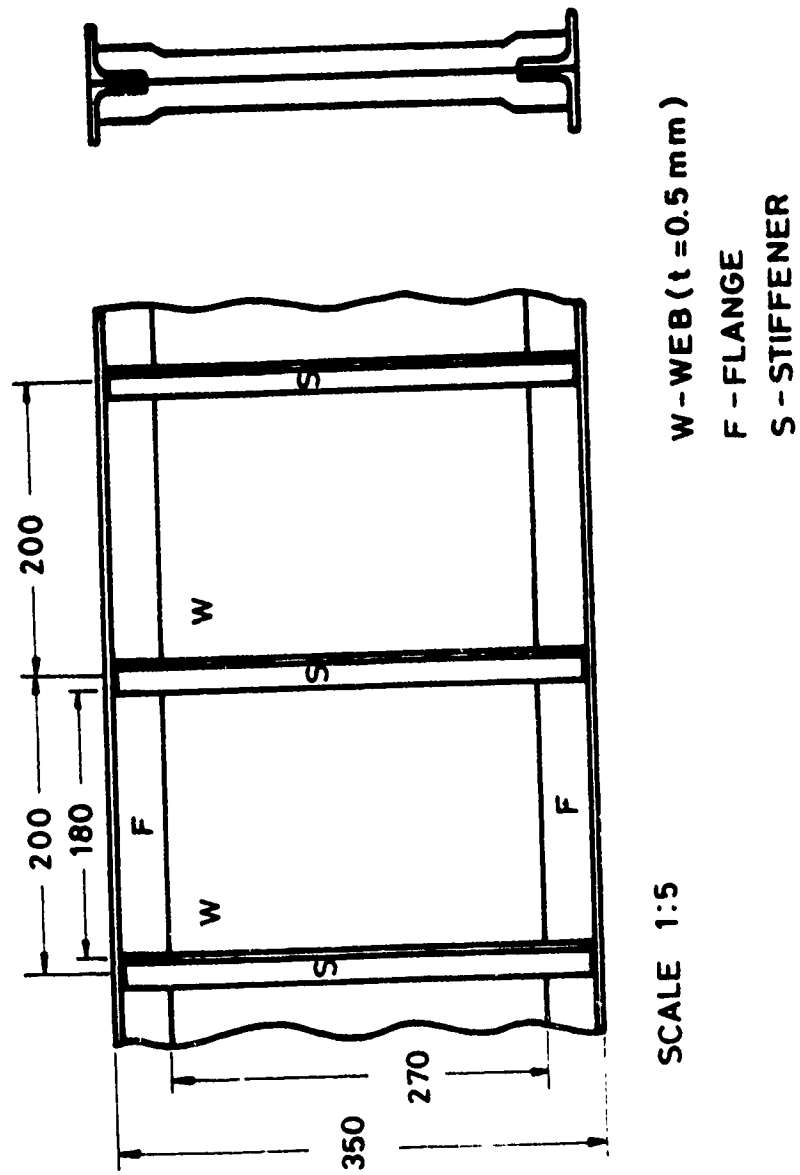S - STIFFENER

SCALE 1:5

Fig. 2   Geometry of stiffened shear panels.
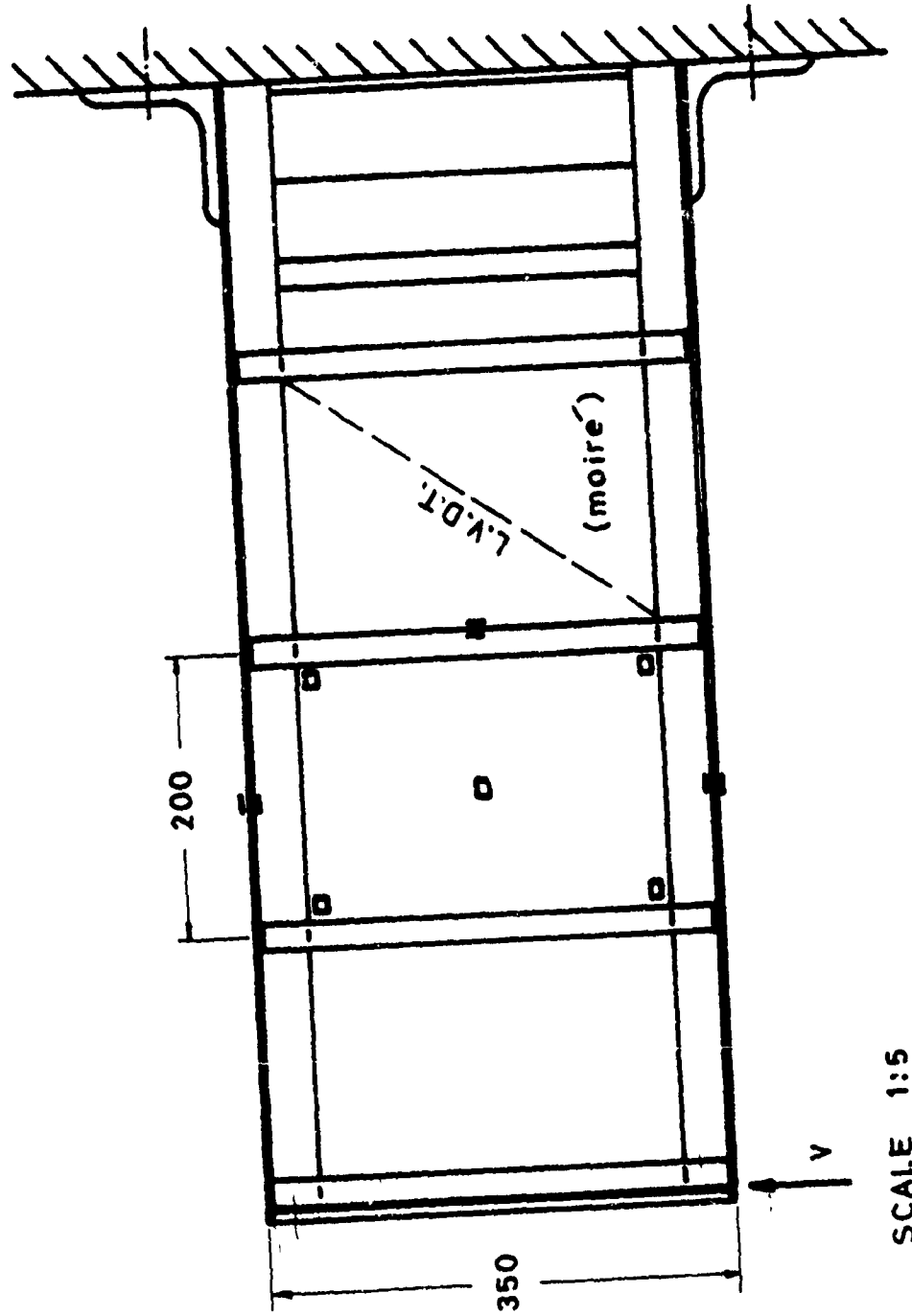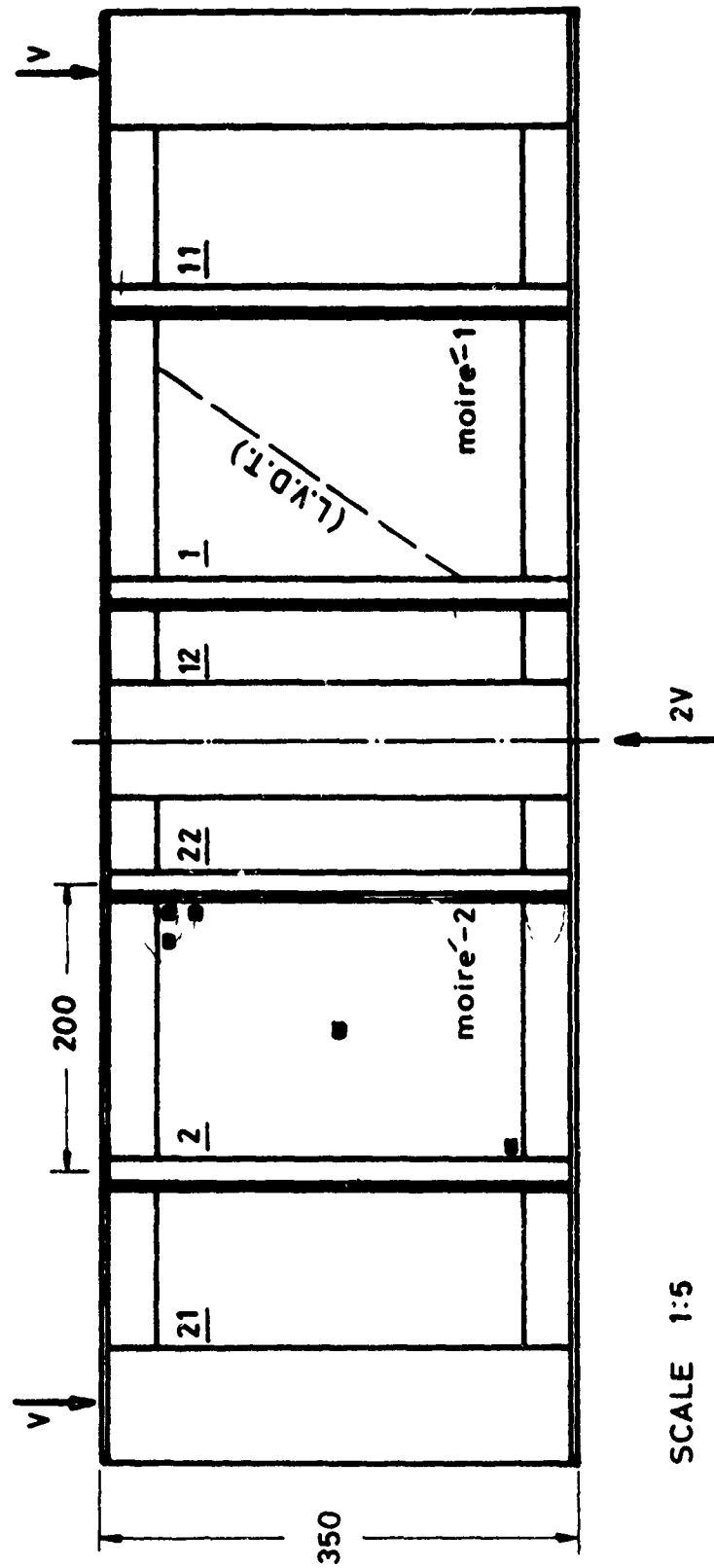
SCALE 1:5

Fig. 3   Wagner Beam WB-01.

SCALE 1:5

Fig. 4   Wagner Beam WB-02.

a. Moiré side.

b. LVDT side.
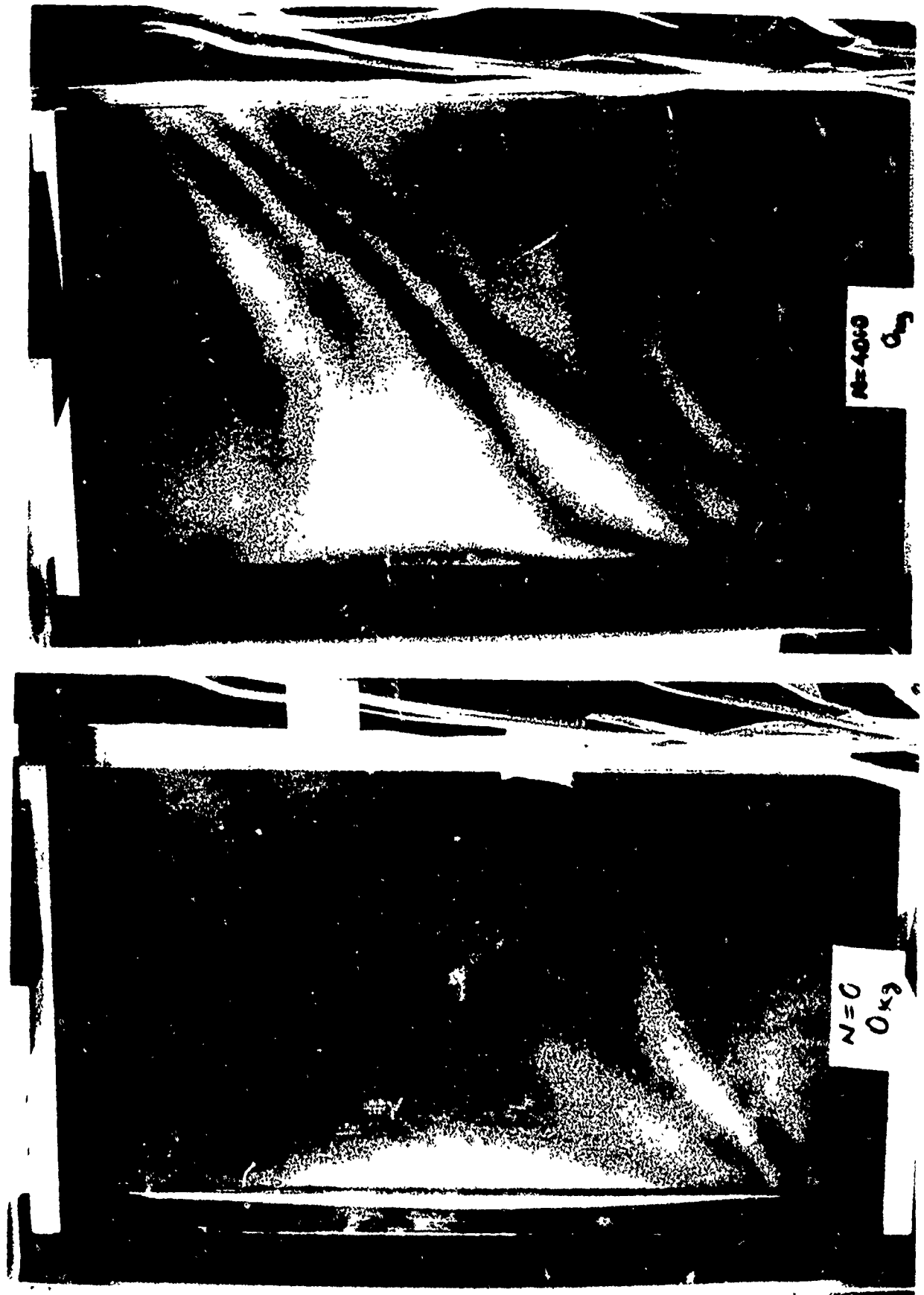
Fig. 5   Two sides of instrumented specimen WB-01.

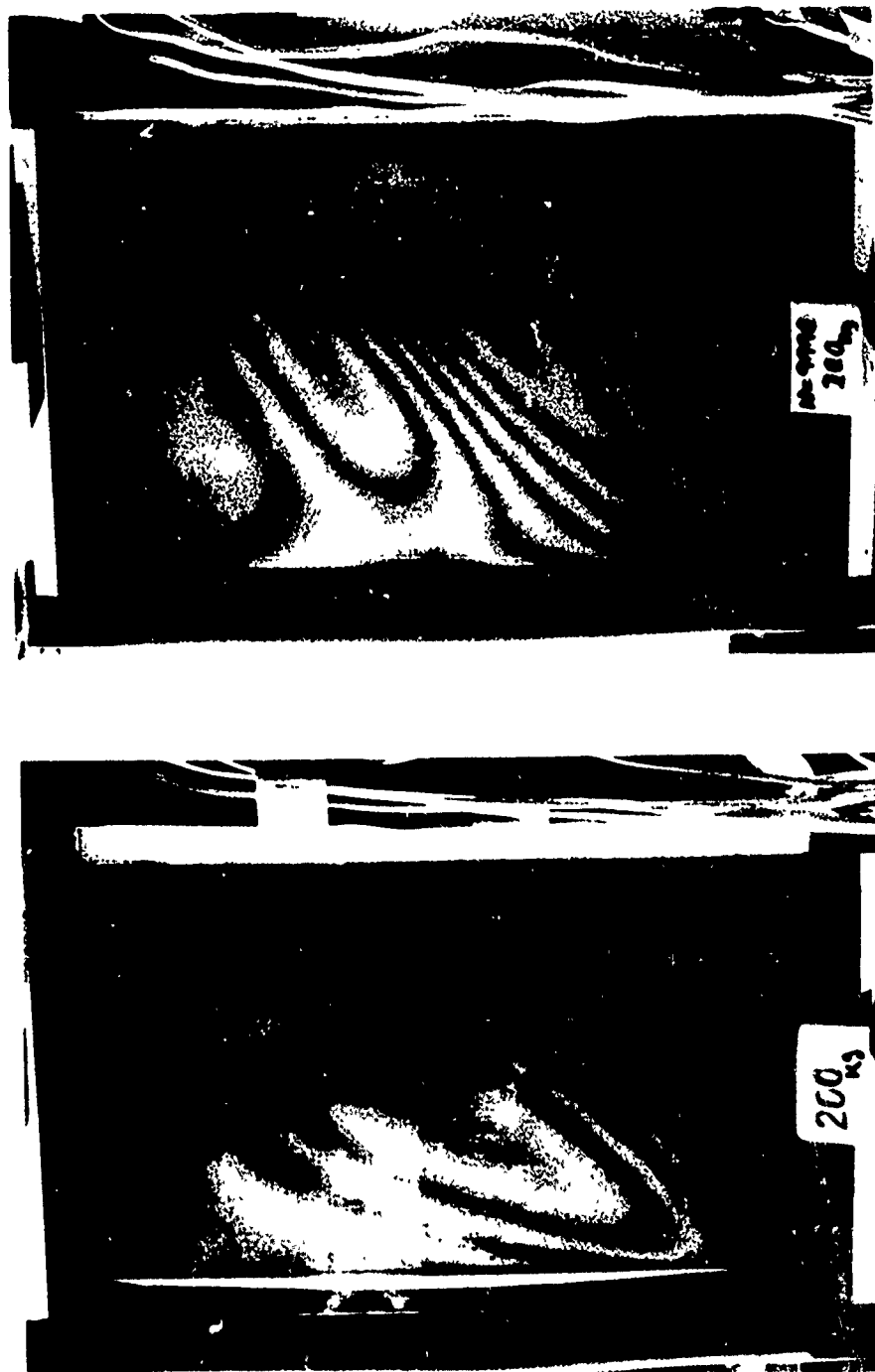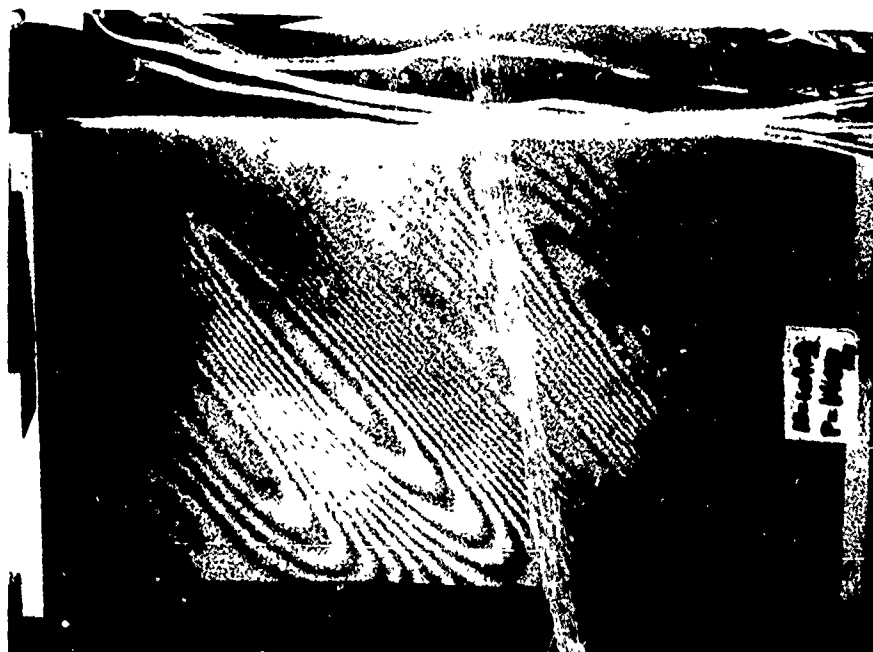Fig. 6   Residual deflections due to cyclic loading (V_{max}=13,73 kN).

Fig. 7 Initial buckling pattern before and after cyclic loading
(V_{max}=13,73 kN).

a. V=13,73kN

b. V=19,62kN

Fig. 8   Buckling patterns at two levels of maximum cyclic load.
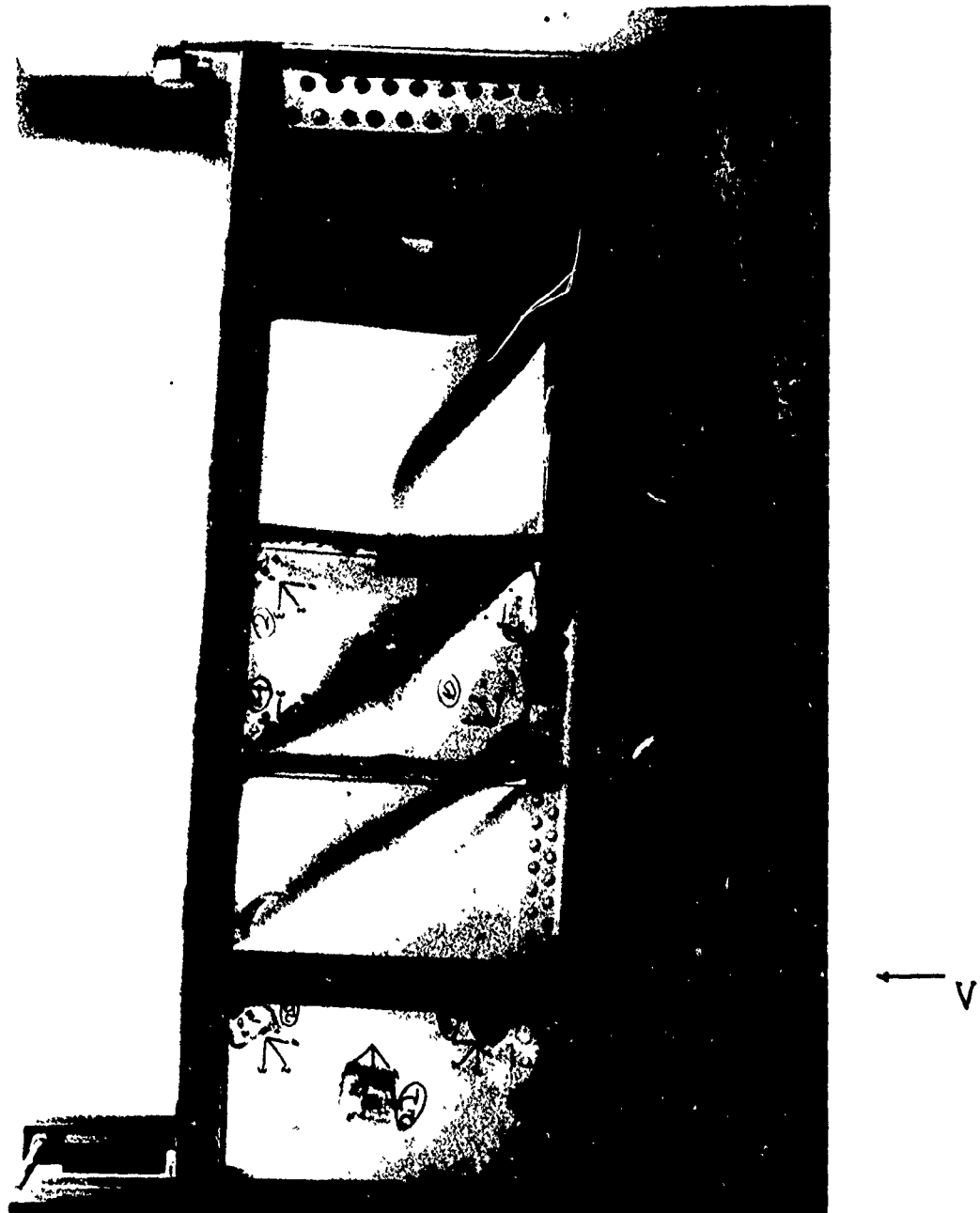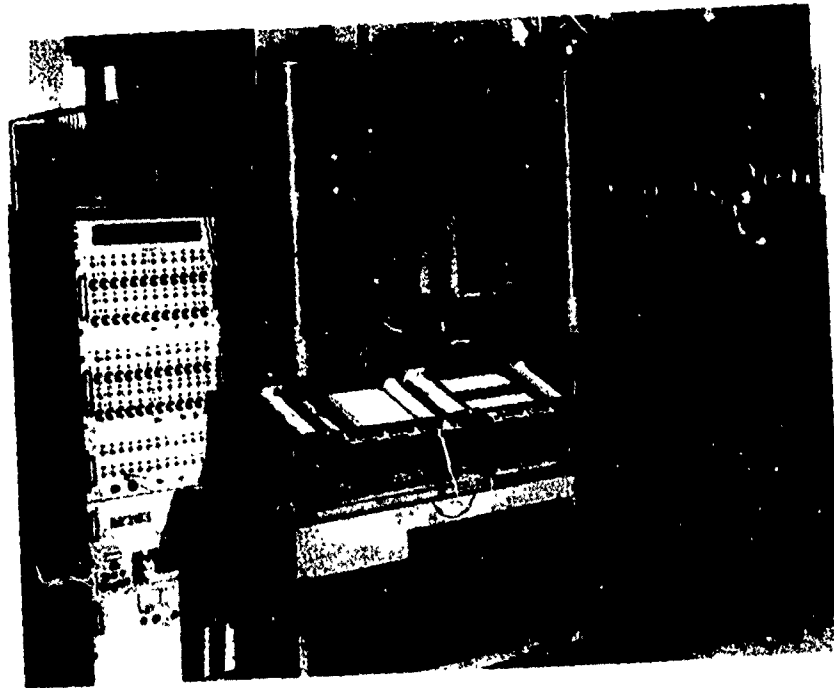
Fig. 9   Failure of Wagner Beam No. 1.

Fig. 10   Test set-up of Wagner Beam No. 2.

a. V = 1.27 kN

b. V = 21.58 kN

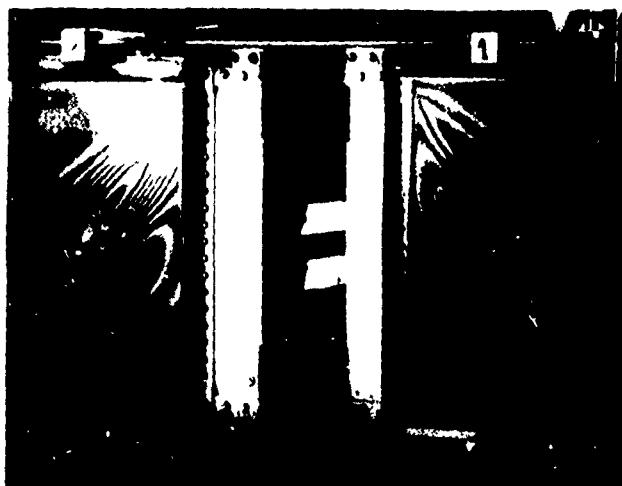Fig. 11   Moire fringes with the two different grid densities at two
load levels.

a. after V = 13,73 kN

b. after V =19,62 kN

c. after V = 21.58 kN

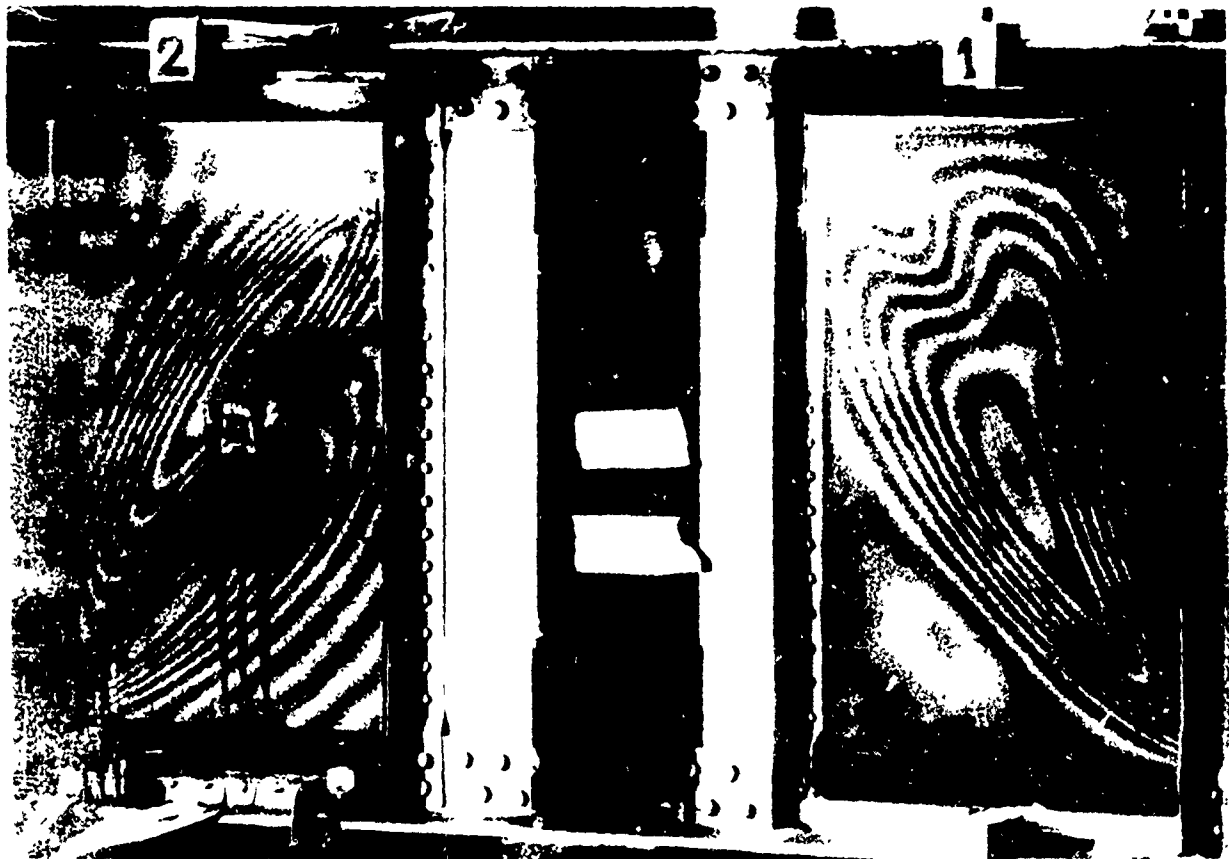Fig. 12 Residual deflections after release of static loading.

Fig. 13   Changed residual deflection after N=2085 load cycles.

Fig. 14   Bending crack along peak of buckling wave at the corner near the
compression flange.

a. LVDT side   b. moire side

Fig. 15   Failure of Wagner Beam No.2.